Eur. Phys. J. B **11**, 235–242 (1999)

THE EUROPEAN PHYSICAL JOURNAL B

EDP Sciences

Doping and temperature dependence of the spin susceptibility in the p-d model

R. Citro[1,a] and M. Marinaro[1,2]

[1] Dipartimento di Scienze Fisiche "E.R. Caianiello", Università di Salerno, 84081 Baronissi (Salerno) and Unità INFM di Salerno, Italy
[2] Istituto Internazionale per gli Alti Studi Scientifici "E.R. Caianiello", IIASS, 84019 Vietri sul Mare (Salerno), Italy

Received 15 October 1998 and Received in final form 24 March 1999

Abstract. The spin magnetic susceptibility of the p-d model is calculated by means of a perturbation theory in the hybridization term V through a generalized cumulant expansion (GCE). The analysis is approached from the paramagnetic metallic phase. The results qualitatively reproduce some unusual magnetic properties in the normal state of the hole-doped cuprates, supporting the scenario of a Van Hove singularity near the Fermi level.

PACS. 74.25.Ha Magnetic properties – 74.72.-h High-T_c compounds – 78.20.Bh Theory, models, and numerical simulation

1 Introduction

The presence of antiferromagnetic correlations in the $Cu-O$ planes of cuprate materials is believed to have important implications for the pairing mechanism in high-T_c superconductors (HTCS). In this context, a study of the magnetic properties of these materials is of some relevance, especially in connection to the normal phase "unusual" magnetic properties experimentally observed. In the case of the $La_{2-x}Sr_xCuO_4$, system, studies of the uniform spin magnetic susceptibility χ_s have shown two properties in the metallic state which might be related to the onset of superconductivity [1,2]:
a) at a fixed temperature, χ_s increases with increasing doping, reaching a maximum in the vicinity of $x \simeq 0.26$, then decreases;
b) at a fixed doping, changing the temperature, χ_s reaches a maximum at a finite temperature T_m that goes to zero as the material is doped with holes near $x \simeq 0.26$.

Similar behaviour has been observed in other ceramic samples as $YBa_2Cu_3O_{6+x}$ [3,4] or $Pb_2Sr_2Y_{1-x}Ca_xO_{6x}Cu_3O_{8+d}$ [5]. An interesting aspect is that some of the cuprate alloys [6] exhibit a nearly T-independent susceptibility above the critical temperature T_c, and the magnitude of χ_s corresponds to a conventional metallic density of states. However, an anomalous decrease in χ_s as T is lowered towards the superconducting transition has been observed [1,7] in numerous cuprates at selected oxygen compositions. This unexplained behaviour provides the primary motivation for the present work.

Based on recent NMR and photoemission spectroscopy data [8,9] a Van Hove scenario for HTCS has been proposed [10,11], in which the above "unusual" magnetic properties are explained in terms of the Fermi level position lying very close to the Van Hove singularity (VHS) in the density of states over a substantial range of doping. Also the direct experimental verifications [12,13] of a "pseudogap" in the density of states of electrons in the metallic layers of cuprate high temperature superconductors in the underdoped regime is considered to be one of the key elements to guide us in the comprehension of the "unusual" properties in these materials. It has been pointed out [14] that a pseudogap structure in the density of states may be relevant to the susceptibility downturn at low T. Furthermore, examples of an upturn in susceptibility at low T have also been discovered [1,15] in certain compositions of cuprates that display metallic transport properties, and such cases present yet another theoretical challenge.

From a theoretical point of view we calculate the spin magnetic susceptibility in the $p-d$ model within a perturbation theory around the atomic limit, based on a generalized cumulant expansion (GCE). We will approach the analysis from the paramagnetic metallic phase rather than the antiferromagnetic case (small x). The goal of the present study is to explain a wide range of anomalous susceptibility variation seen in cuprates in terms of a simple Van Hove singularity of the electronic density of states, which arises from the nearest neighbour hybridization term between the p and d orbitals in the CuO_2 planes.

[a] *Present address*: Department of Physics, Rutgers University, Piscataway, New Jersey 08855-0849, USA.
e-mail: citro@vaxsa.csied.unisa.it

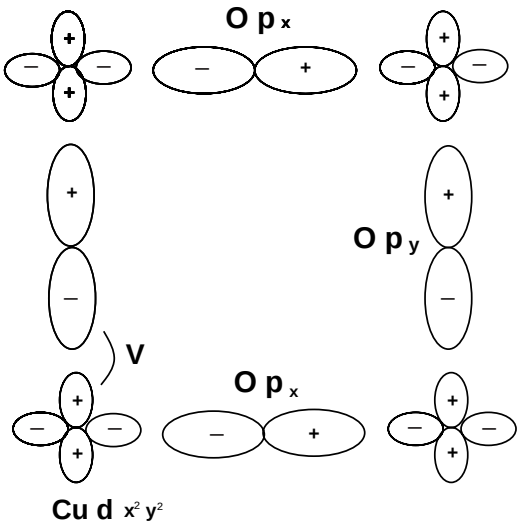

Fig. 1. Orbitals and hopping term included in the p-d model Hamiltonian.

In the approach presented here, the local part of the Hamiltonian containing the on-site Coulomb repulsion U_d is solved exactly and the hybridization term is introduced as a perturbation. We can point out such a merit of this perturbative approach that it is expected to describe the normal state in the intermediate and large-U regime more accurately than a simple tight-binding approach [16] or a weak coupling perturbation theory [17]. In this sense, it is useful to study how correlation effects modify the behavior of the physical quantities in the Fermi-liquid phase and cause anomalous behavior. Moreover, the approach is free from size effects compared with numerical simulations, and situable for the description of the low-energy properties and the phase transition such as metal-insulator transitions (MIT). On the other hand, there exists the drawback that by introducing the hybridization term as a perturbation, the presence of the Coulomb interaction term in the atomic Hamiltonian prevents the application of the Wick decoupling procedure, and a GCE has to be introduced.

In order to evaluate the spin susceptibility we utilize a Bethe-Salpeter equation for the vertex functions taking into account the correlation effects through the inclusion of the cumulants of the first and second order. The calculation is performed in the framework of the well-known finite temperature Green's function formalism.

2 The model Hamiltonian

Taking into account the characteristic feature of the CuO_2 plane, we adopt the p-d model. In this model, tight-binding holes are composed of $Cu-d_{x^2-y^2}$ orbitals which form a square lattice and O-p_α ($\alpha = x, y$) orbitals which connect the nearest-neighbour Cu sites (see Fig. 1).

The non-interacting part of the Hamiltonian consists of site energy terms of d- and p-orbitals and the Coulomb repulsion U_d on each d-orbital. As for the interaction, we consider the transfer term between nearest-neighbor d- and p-orbitals. Thus we obtain the following Hamiltonian,

$$H = H_0 + H_1 \tag{1}$$

where

$$H_0 = (\varepsilon_p - \mu)\sum_{\mathbf{k},\sigma} p^\dagger_{\mathbf{k}\sigma} p_{\mathbf{k}\sigma} + (\varepsilon_d - \mu)\sum_{\mathbf{k},\sigma} d^\dagger_{\mathbf{k}\sigma} d_{\mathbf{k}\sigma} + \frac{U_d}{N}\sum_{\mathbf{k},\mathbf{k}'}\sum_{\mathbf{q}(\neq\mathbf{0})} d^\dagger_{\mathbf{k}+\mathbf{q}\uparrow} d^\dagger_{\mathbf{k}'-\mathbf{q}\downarrow} d_{\mathbf{k}'\downarrow} d_{\mathbf{k}\uparrow} \tag{2}$$

$$H_1 = \sum_{\mathbf{k},\sigma} V_{\mathbf{k}} (d^\dagger_{\mathbf{k}\sigma} p_{\mathbf{k}\sigma} + \text{h.c.}), \tag{3}$$

where $d^\dagger_{\mathbf{k}\sigma}(d_{\mathbf{k}\sigma})$ and $p^\dagger_{\mathbf{k}\sigma}(p_{\mathbf{k}\sigma})$ are the creation (annihilation) operator for d- and p- holes of momentum $\mathbf{k}$ and spin σ, respectively. The site energy of d- and p-holes are given by $(\varepsilon_d - \mu)$ and $(\varepsilon_p - \mu)$, μ is the chemical potential. Finally, U_d represents the on-site Coulomb repulsion between Cu holes. The bonding orbital $p_{\mathbf{k}\sigma}$, hybridizing with the $d_{\mathbf{k}\sigma}$, orbital is given by the following combination of $p_{x\mathbf{k}\sigma}$ and $p_{y\mathbf{k}\sigma}$ orbitals:

$$p_{\mathbf{k}\sigma} = \left(\frac{\gamma_{k_x}}{\gamma_{\mathbf{k}}} p_{x\mathbf{k}\sigma} - \frac{\gamma_{k_y}}{\gamma_{\mathbf{k}}} p_{y\mathbf{k}\sigma}\right), \tag{4}$$

where $\gamma_{k_\alpha} = \sin(k_\alpha/2)$, $(\alpha = x, y)$. The p-d mixing term is given by

$$V^2_{\mathbf{k}} = 2V^2(2 - \cos k_x - \cos k_y) = 2V\gamma(\mathbf{k}), \tag{5}$$

where V is the p-d hybridization. In the following calculation, we put $V = 1$. The typical order of energy V is ~ 1 eV, that is $\sim 10^4$ K.

Denoting by H_0 the atomic part of the Hamiltonian (1) and by H_1 the hybridization term, the Green's functions for p and d operators, at temperature different from zero, are determined through the standard S-matrix perturbative formula

$$G_{\alpha\beta}(i-j, \tau_1 - \tau_2) = -\frac{\left\langle T_\tau c^\alpha_{i\sigma}(\tau_1) c^{\beta\dagger}_{i\sigma}(\tau_2) S(\beta)\right\rangle_0}{\langle S(\beta)\rangle_0}, \tag{6}$$

where the underscript (α, β) represents either p- or d-hole indices and $S(\beta)$ is given by

$$S(\beta) = \sum_{n=0}^{\infty} \frac{(-1)^n}{n!} \int_0^\beta \mathrm{d}\tau_1 \int_0^\beta \mathrm{d}\tau_2 \ldots\ldots \int_0^\beta \mathrm{d}\tau_n \times T_\tau(H_1(\tau_1)\cdots\cdots H_1(\tau_n)). \tag{7}$$

The unperturbed atomic single-particle Green's functions $G^{(0)}_{pp}$ and $G^{(0)}_{dd}$ are given by:

$$G^{(0)}_{pp}(\mathrm{i}\omega_\nu) = \frac{1}{\mathrm{i}\omega_\nu - (\varepsilon_p - \mu)} \tag{8}$$

and

$$G^{(0)}_{dd}(\mathrm{i}\omega_\nu) = \frac{(1 - \langle n^d_{\bar\sigma}\rangle_0)}{\mathrm{i}\omega_\nu - (\varepsilon_d - \mu)} + \frac{\langle n^d_{\bar\sigma}\rangle_0}{\mathrm{i}\omega_\nu - (\varepsilon_d + U - \mu)}, \tag{9}$$

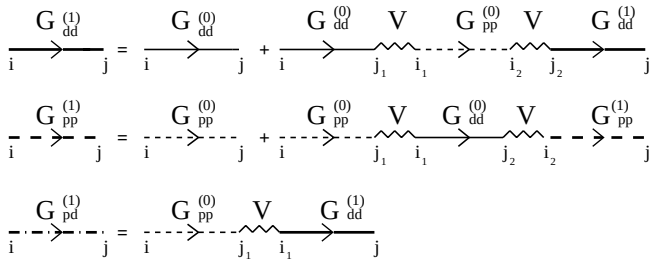

Fig. 2. Chain-like diagrams for the one-particle Green's functions. The thin solid and dashed lines, respectively, indicate the bare Green's functions $G^{(0)}_{dd}(i-j)$ and $G^{(0)}_{pp}(i-j)$, while the wavey line represents the hybridization V_{ij}.

where ω_ν are the fermion Matsubara frequencies at a temperature T, and $\langle n^d_{\bar\sigma}\rangle_0$ is the average number of particles with spin $\bar\sigma$ in the d-atomic orbital. In calculating the full Green's functions (6), since H_0 does not mix p and d operators, the thermal averages appearing in the expansion can be expressed as products of p- and d-averages, separately. While the p-averages may be evaluated using the conventional Wick decoupling scheme, the presence of the Coulomb interaction term (U_d) in H_0 prevents the application to the d-averages of this procedure. For this reason, one can apply a nonstandard diagrammatic expansion, analogous to that developed by Metzner [18] for the one-band Hubbard model. Within this approach, the simplest approximation consists in decoupling the d-averages of four or more fermionic operators in products of local pair averages, or equivalently, in taking into account only the single-site one-particle cumulants. Diagrammatically, in this approximation, one obtains the chain-like diagrams (shown in Fig. 2) which can be summed up by means of a Dyson-like equation leading for $G^{(1)}_{pp}, G^{(1)}_{dd}, G^{(1)}_{pd}$ to the expressions:

$$G^{(1)}_{pp}(\mathbf{k}, \mathrm{i}\omega_\nu) = \frac{G^{(0)}_{pp}(\mathrm{i}\omega_\nu)}{1 - V^2_{\mathbf{k}} G^{(0)}_{pp}(\mathrm{i}\omega_\nu) G^{(0)}_{dd}(\mathrm{i}\omega_\nu)} \tag{10}$$

$$G^{(1)}_{dd}(\mathbf{k}, \mathrm{i}\omega_\nu) = \frac{G^{(0)}_{dd}(\mathrm{i}\omega_\nu)}{1 - V^2_{\mathbf{k}} G^{(0)}_{pp}(\mathrm{i}\omega_\nu) G^{(0)}_{dd}(\mathrm{i}\omega_\nu)} \tag{11}$$

$$G^{(1)}_{pd}(\mathbf{k}, \mathrm{i}\omega_\nu) = G^{(0)}_{pp}(\mathrm{i}\omega_\nu) V_{\mathbf{k}} G^{(1)}_{dd}(\mathbf{k}, \mathrm{i}\omega_\nu). \tag{12}$$

We call this approximation the "first-order cumulant expansion" [19–21].

Although starting from the atomic limit, the Green's function (10–12) obtained by selecting chain-like diagrams and summing up the whole series, present a large Fermi-surface having loosed completely its atomic character. Therefore, according to experimental data, it seems appropriate to compute the physical quantities in the optimal and overdoped regime (large x), rather than the antiferromagnetic (AF) phase (small x). In fact, in this phase the approximation used underrates the p-d spin fluctuations *a la* Zhang-Rice which dominate the physics in the quasi-atomic limit.

The average number of particles in both p- and d- orbitals is determined together with the chemical potential, through the self-consistency relation:

$$\langle n^\alpha_\sigma \rangle = \lim_{\varepsilon\to 0} \beta^{-1} \sum_{\omega_\nu} \mathrm{e}^{\mathrm{i}\omega_\nu \varepsilon} \frac{1}{N} \sum_{\mathbf{k}\sigma} G_{\alpha\alpha,\sigma}(\mathbf{k}, \mathrm{i}\omega_\nu). \tag{13}$$

Finally, remembering that spin magnetic susceptibility reflects the thermal averages of the density of states (DOS) at the Fermi level, in order to interpret the results of χ_s and to investigate the role played by the presence of a sharp feature in it, the DOS for a given spin direction has been evaluated as a function of the energy from the knowledge of the one-particle Green's functions, by means of the following relation:

$$\begin{aligned}\rho_\sigma(\omega) &= -\frac{1}{\pi}\mathrm{Im} \sum_{\mathbf{k}} \Big[G^{(1)}_{pp\sigma}(\mathbf{k}, \omega_n \to \omega + \mathrm{i}\eta) \\ &\quad + G^{(1)}_{dd\sigma}(\mathbf{k}, \omega_n \to \omega + \mathrm{i}\eta) \Big] \\ &= \sum_{i=1}^{3} \int \frac{\mathrm{d}^2 k}{(2\pi)^2} \left[A_i(\mathbf{k}) + B_i(\mathbf{k}) \right] \delta\left(\omega - (E_i(\mathbf{k}) - \mu)\right)\end{aligned} \tag{14}$$

where $(E_i(\mathbf{k}) - \mu)$ are the energy spectra calculated from the poles of the Green's functions (Eqs. (10, 11)) and $A_i(\mathbf{k})$, $B_i(\mathbf{k})$ are the corresponding residues. We note that all these quantities depend on $\mathbf{k}$ through the term $V^2(\mathbf{k})$ from equation (5). Thus equation (14) can be written in terms of a one-dimensional integral as

$$\begin{aligned}\rho_\sigma(\omega) = \frac{2}{\pi^2} \sum_{i=1}^{3} \int_{-1}^{1} \mathrm{d}x K\left(\sqrt{1-x^2}\right) \\ \times \left[A_i(x) + B_i(x) \right] \delta\left(\omega - (E_i(x) - \mu)\right),\end{aligned} \tag{15}$$

where $K\left(\sqrt{1-x^2}\right)$ is the complete elliptic integral of the first type.

3 The spin susceptibility

We define the spin susceptibility, $\chi^{\alpha\beta}_\mathrm{s}(\mathbf{q}, \mathrm{i}\omega_\upsilon)$, as

$$\chi^{\alpha\beta}_\mathrm{s}(\mathbf{q}, \mathrm{i}\omega_\upsilon) = (g\mu_B)^2 \int_0^\beta \mathrm{d}\tau \mathrm{e}^{\mathrm{i}\omega_\upsilon \tau} \langle T_\tau [S^{z\alpha}_{\mathbf{q}}(\tau) S^{z\beta}_{-\mathbf{q}}(0)] \rangle \tag{16}$$

where the superscript (α, β) represents p- and d- hole indices, and $S^z_{\mathbf{q}}$ is given by

$$S^z_{\mathbf{q}} = \frac{1}{2} \sum_{\mathbf{k}} [c^\dagger_{\mathbf{k}+\mathbf{q}\uparrow} c_{\mathbf{k}\uparrow} - c^\dagger_{\mathbf{k}+\mathbf{q}\downarrow} c_{\mathbf{k}\downarrow}] = \frac{1}{2}(n_{\mathbf{q}\uparrow} - n_{\mathbf{q}\downarrow}) \tag{17}$$

with $n_{\mathbf{q}} = \sum_{\mathbf{k},\sigma} c^\dagger_{\mathbf{k}+\mathbf{q}\sigma} c_{\mathbf{k}\sigma}$. Here, g is the Landè factor and μ_B is the Bohr magneton. The magnetic unit is fixed as $g\mu_\mathrm{B}/2 = 1$.

Equation (16) can be recast into

$$\chi_s^{\alpha\beta}(\mathbf{q}, \mathrm{i}\omega_\upsilon) = 2\left[\chi_{\uparrow\uparrow}^{\alpha\beta}(\mathbf{q}, \mathrm{i}\omega_\upsilon) - \chi_{\downarrow\uparrow}^{\alpha\beta}(\mathbf{q}, \mathrm{i}\omega_\upsilon)\right], \quad (18)$$

where $\chi_{\sigma\sigma'}^{\alpha\beta}(\mathbf{q}, \mathrm{i}\omega_\upsilon)$ is the generalized susceptibility in the "particle-hole" channel, defined as

$$\chi_{\sigma\sigma'}^{\alpha\beta}(\mathbf{q}, \mathrm{i}\omega_\upsilon) = \int_0^\beta \mathrm{d}\tau \mathrm{e}^{\mathrm{i}\omega_\upsilon\tau} \langle T_\tau \sum_{\mathbf{k}} c_{\mathbf{k}+\mathbf{q}\sigma}^{\alpha\dagger}(\tau) c_{\mathbf{k}\sigma}^{\beta}(\tau) \times \sum_{\mathbf{p}} c_{\mathbf{p}+\mathbf{q}\sigma'}^{\alpha\dagger}(0) c_{\mathbf{p}\sigma'}^{\beta}(0)\rangle^{\mathrm{conn}}, \quad (19)$$

in which the superscript "conn" denotes the operation to take into account only the connected diagrams. The total susceptibility will be obtained by summing up the four contributions $\chi_{\sigma\sigma'}^{pp}, \chi_{\sigma\sigma'}^{dd}, \chi_{\sigma\sigma'}^{dp}$, and $\chi_{\sigma\sigma'}^{pd}$. In expanding the right side of equation (19) with respect to the hybridization term, we pass first from the delocalized to the site representation for the fermion operators, *via* the definition

$$c_{\mathbf{k}\sigma} = \frac{1}{\sqrt{N}} \sum_i c_{i\sigma} \mathrm{e}^{\mathrm{i}\mathbf{k}\cdot\mathbf{R}_i}. \quad (20)$$

In this way the problem of evaluating the generalized susceptibility is reduced to the calculation of a two-particle Green's function $G_2^{\alpha\beta}(i\sigma\tau, j\sigma'0 \mid i\sigma\tau, j\sigma'0)$. This two-particle Green's function can be expressed in terms of the single-particle propagators and the "irreducible" part by writing

$$G_2(i\sigma\tau, j\sigma'0 \mid i\sigma\tau, j\sigma'0) = G_1(i\sigma\tau)G_1(j\sigma'0) - G_1(i\sigma\tau \mid j\sigma'0)G_1(j\sigma'0 \mid i\sigma\tau)\delta_{\sigma\sigma'} + G_2^{\mathrm{irr}}(i\sigma\tau, j\sigma'0 \mid i\sigma\tau, j\sigma'0). \quad (21)$$

The first term on the right of equation (21) does not contribute to equation (19). For the remaining two's, the product of the one-particle Green's functions correspond to an Hartree-Fock term, while G_2^{irr}, contains the vertex-corrections. The Hartree-Fock term provides "bubble-diagrams" to $\chi_{\sigma\sigma}^{\alpha\beta}$ (see Fig. 3), whose analytic expression in terms of the Green's functions (10–12), for a fixed spin direction, is given by

$$\chi_{\uparrow\uparrow}^{(1)\alpha\beta}(\mathbf{q}, \mathrm{i}\omega_\upsilon) = -\beta^{-1} \sum_{\Omega_\nu} \mathrm{e}^{\mathrm{i}\Omega_\nu\varepsilon} \times \int \frac{\mathrm{d}^2k}{(2\pi)^2} G_{\uparrow\alpha\beta}^{(1)}(\mathbf{k}+\mathbf{q}, \mathrm{i}\omega_\upsilon + \mathrm{i}\Omega_\nu) G_{\uparrow\alpha\beta}^{(1)}(\mathbf{k}, \mathrm{i}\Omega_\nu). \quad (22)$$

In calculating the irreducible part of $\chi_{\sigma\sigma'}^{\alpha\beta}$, we first introduce the d- vertex function:

$$\Gamma_{\sigma\sigma'}(\mathbf{q}, \mathrm{i}\omega_\upsilon) = \int_0^\beta \mathrm{d}\tau \mathrm{e}^{\mathrm{i}\omega_\upsilon\tau} \times \langle T_\tau(d_{\mathbf{k}+\mathbf{q}\sigma}^\dagger(\tau) d_{\mathbf{k}\sigma}(\tau) d_{\mathbf{k}+\mathbf{q}\sigma}^\dagger(0) d_{\mathbf{k}\sigma}(0))\rangle^{\mathrm{conn}} \quad (23)$$

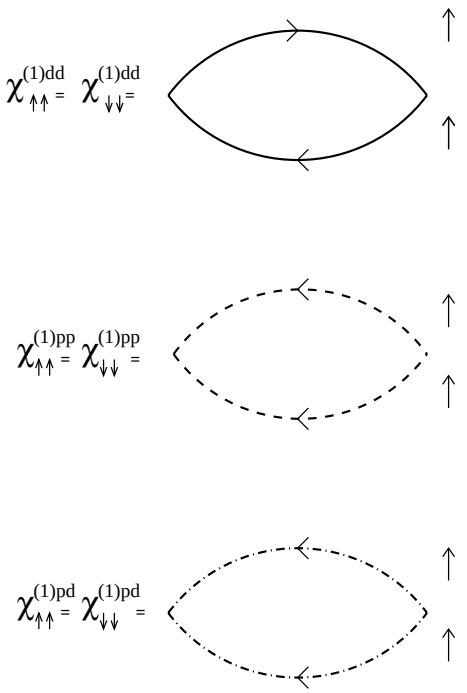

Fig. 3. Diagrams for the Hartree-Fock term in $\chi_{\sigma\sigma'}^{\alpha\beta}$. The solid, dashed and dashed-dotted lines indicate the Green's functions $G_{dd}^{(1)}(i-j)$, $G_{pp}^{(1)}(i-j)$ and $G_{pd}^{(1)}(i-j)$ in the chain-like approximation.

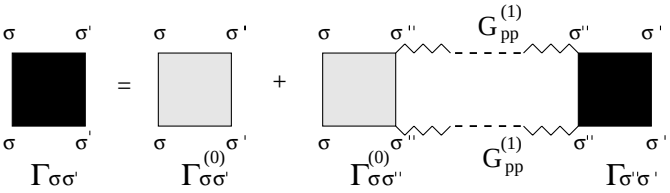

Fig. 4. Diagrammatic representation of the Bethe-Salpeter equation for the vertex function $\Gamma_{\sigma\sigma'}$ in the particle-hole channel.

that can be determined from the Bethe-Salpeter equation (see Fig. 4)

$$\Gamma_{\sigma\sigma'}(\mathbf{q}, \mathrm{i}\omega_\upsilon) = \Gamma_{\sigma\sigma'}^{(0)}(\mathrm{i}\omega_\upsilon) + \sum_{\sigma''} \Gamma_{\sigma\sigma''}^{(0)}(\mathrm{i}\omega_\upsilon) \Pi_{\sigma''}^{pp}(\mathbf{q}, \mathrm{i}\omega_\nu) \Gamma_{\sigma''\sigma'}(\mathbf{q}, \mathrm{i}\omega_\upsilon), \quad (24)$$

where $\Gamma_{\sigma\sigma'}^{(0)}(\mathrm{i}\omega_\upsilon)$ is the irreducible vertex function (*i.e.* a two-particle single-site cumulant) for the d-holes

$$\Gamma_{\sigma\sigma'}^{(0)}(\mathrm{i}\omega_\upsilon) = \int_0^\beta \mathrm{d}\tau \mathrm{e}^{\mathrm{i}\omega_\upsilon\tau} \times \langle T_\tau(d_{\mathbf{k}+\mathbf{q}\sigma}^\dagger(\tau) d_{\mathbf{k}\sigma}(\tau) d_{\mathbf{k}+\mathbf{q}\sigma}^\dagger(0) d_{\mathbf{k}\sigma}(0))\rangle_0^{\mathrm{irr}}, \quad (25)$$

in which the average is performed with respect to the atomic Hamiltonian H_0 and $\Pi_\sigma^{pp}(\mathbf{q}, \mathrm{i}\omega_\nu)$ is

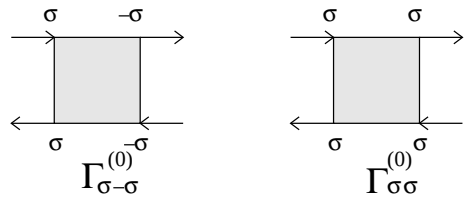

Fig. 5. Irreducible vertex $\Gamma^{(0)}_{\sigma\sigma'}$ for the two possible choices of the spin variables in the particle-hole channel.

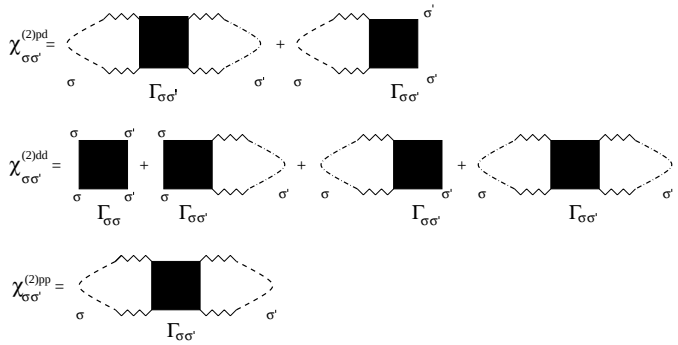

Fig. 6. Diagrams for $\chi_{\sigma\sigma'}$ within second order cumulant expansion.

the polarization insertion

$$\Pi^{pp}_{\sigma}(\mathbf{q}, \mathrm{i}\omega_\nu) = -\beta^{-1} \sum_{\Omega_\nu} \mathrm{e}^{\mathrm{i}\Omega_\nu \varepsilon} \int \frac{\mathrm{d}^2 k}{(2\pi)^2} V^2(\mathbf{k}+\mathbf{q}) \times G^{(1)}_{\sigma pp}(\mathbf{k}+\mathbf{q}, \mathrm{i}\omega_\upsilon + \mathrm{i}\Omega_\nu) V^2(\mathbf{k}) G^{(1)}_{\sigma pp}(\mathbf{k}, \mathrm{i}\Omega_\nu).$$

The expressions for the irreducible vertex [22], represented in Figure 5 in correspondence of the two-possible spin choices in the particle-hole channel, are reported in Table 1. The contribution to $\chi^{(2)\alpha\beta}_{\sigma\sigma'}(\mathbf{q}, \mathrm{i}\omega_\upsilon)$ coming from equation (23) is diagrammatically shown in Figure 6 and analytically given by

$$\chi^{(2)dd}_{\sigma\sigma'}(\mathbf{q}, \mathrm{i}\omega_\upsilon) = \Gamma_{\sigma\sigma'}(\mathbf{q}, \mathrm{i}\omega_\upsilon) \left[1 + \tilde{\Pi}^{pd}_{\sigma'}(\mathbf{q}, \mathrm{i}\omega_\nu)\right]^2 \quad (26)$$

$$\chi^{(2)pp}_{\sigma\sigma'}(\mathbf{q}, \mathrm{i}\omega_\upsilon) = \Gamma_{\sigma\sigma'}(\mathbf{q}, \mathrm{i}\omega_\upsilon) \tilde{\Pi}^{pp2}_{\sigma'}(\mathbf{q}, \mathrm{i}\omega_\nu) \quad (27)$$

$$\chi^{(2)pd}_{\sigma\sigma'}(\mathbf{q}, \mathrm{i}\omega_\upsilon) = \chi^{(2)dp}_{\sigma\sigma'}(\mathbf{q}, \mathrm{i}\omega_\upsilon) = \Gamma_{\sigma\sigma'}(\mathbf{q}, \mathrm{i}\omega_\upsilon) \tilde{\Pi}^{pp}_{\sigma'}(\mathbf{q}, \mathrm{i}\omega_\nu) \left[1 + \tilde{\Pi}^{pd}_{\sigma'}(\mathbf{q}, \mathrm{i}\omega_\nu)\right], \quad (28)$$

where

$$\tilde{\Pi}^{\alpha\beta}_{\sigma}(\mathbf{q}, \mathrm{i}\omega_\nu) = -\beta^{-1} \sum_{\Omega_\nu} \mathrm{e}^{\mathrm{i}\Omega_\nu \varepsilon} \int \frac{\mathrm{d}^2 k}{(2\pi)^2} V(\mathbf{k}+\mathbf{q}) \times G^{(1)}_{\sigma\alpha\beta}(\mathbf{k}+\mathbf{q}, \mathrm{i}\omega_\upsilon + \mathrm{i}\Omega_\nu) V(\mathbf{k}) G^{(1)}_{\sigma\alpha\beta}(\mathbf{k}, \mathrm{i}\Omega_\nu).$$

The superscript $^{(2)}$ indicates that we are taking into account the two-particle cumulants contained in the irreducible part. We call this approximation the "second-order cumulant expansion" (SOCE). Combining equation (18) with the explicit expressions of $\chi^{\alpha\beta}_{\sigma\sigma'}(\mathbf{q}, \mathrm{i}\omega_\upsilon) = \chi^{(1)\alpha\beta}_{\sigma\sigma'}(\mathbf{q}, \mathrm{i}\omega_\upsilon) + \chi^{(2)\alpha\beta}_{\sigma\sigma'}(\mathbf{q}, \mathrm{i}\omega_\upsilon)$ from equation (22) and equations (26–28), we obtain $\chi_{\mathrm{s}}(\mathbf{q}, \mathrm{i}\omega_\upsilon)$ in the form

$$\chi_{\mathrm{s}}(\mathbf{q}, \mathrm{i}\omega_\upsilon) = -2\beta^{-1} \sum_{\alpha\beta} \sum_{\Omega_\nu} \mathrm{e}^{\mathrm{i}\Omega_\nu \varepsilon} \int \frac{\mathrm{d}^2 k}{(2\pi)^2} \times G^{(1)\alpha\beta}_{\uparrow}(\mathbf{k}+\mathbf{q}, \mathrm{i}\omega_\upsilon + \mathrm{i}\Omega_\nu) G^{(1)\alpha\beta}_{\uparrow}(\mathbf{k}, \mathrm{i}\Omega_\nu) + 2(\Gamma_{\uparrow\uparrow} - \Gamma_{\uparrow\downarrow})(\mathbf{q}, \mathrm{i}\omega_\upsilon) \left[1 + \tilde{\Pi}^{pd}_{\uparrow}(\mathbf{q}, \mathrm{i}\omega_\nu) + \tilde{\Pi}^{pp}_{\uparrow}(\mathbf{q}, \mathrm{i}\omega_\nu)\right]^2. \quad (29)$$

We would like to stress that the "bubble"-diagrams' contributions, proportional to the single-particle Green's functions product, become relevant in the small-U limit and survive for $U_d = 0$. This means the approach is appropriate not only to describe the physical quantities in the large-U limit (strong-coupling regime), but also to recover the proper behavior in the noninteracting limit.

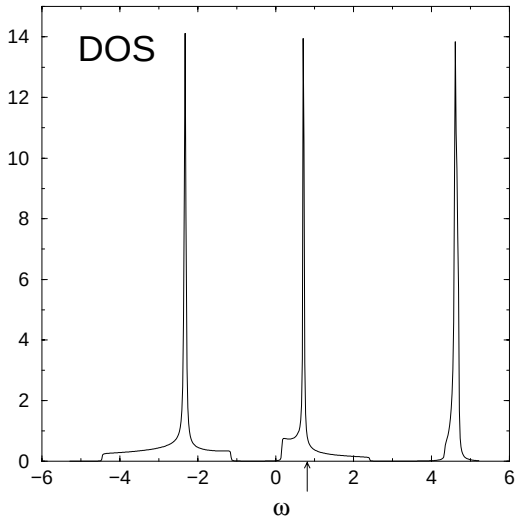

Fig. 7. The density of states as a function of the energy ω for $T = 100$ K, $U_d/V = 5$ and $\varepsilon_d/V = -1$. The arrow indicates the position of the Fermi level for $x = 0.26$.

4 Doping and temperature dependence of the spin susceptibility

In Figure 7 the density of states (DOS) calculated through relations (14, 15) is plotted as a function of the energy ω, having fixed the temperature at $T = 100$ K and for the parameters $U_d/V = 5$, $\varepsilon_d/V = -1$ and $\varepsilon_p/V = 0$. The DOS presents three sharp peaks around the atomic levels ε_d, ε_p and $\varepsilon_d + U$. The sharpness of the peaks reflects the VHS introduced by the nearest-neighbours hopping term. The arrow indicates the Fermi level position E_{F} in correspondence of the hole density $x = 0.26$. At increased doping, E_{F} approaches the VHS and lies on it at $x = x_{\mathrm{c}} \simeq 0.26$, then moves away from it for $x > x_{\mathrm{c}}$. As shown, due to the presence of strong-correlation effects, the VHS is not

Table 1.

Irreducible vertices in the particle-hole channel
$\Gamma^{(0)}_{\sigma\bar{\sigma}}(\mathrm{i}\omega_\nu) = \left[\frac{1}{Z_d}\mathrm{e}^{-\beta(2(\varepsilon_d-\mu)+U_d)} - \left\langle n^d_{\bar{\sigma}}\right\rangle^2\right]\delta(\omega_\nu)$
$\Gamma^{(0)}_{\sigma\sigma}(\mathrm{i}\omega_\nu) = \left[\left\langle n^d_{\bar{\sigma}}\right\rangle\left(1-\left\langle n^d_{\bar{\sigma}}\right\rangle\right) - \frac{1}{Z_d^2}\mathrm{e}^{-\beta(\varepsilon_d-\mu)}(1+\mathrm{e}^{-\beta(2(\varepsilon_d-\mu)+U_d)})\right]\delta(\omega_\nu)$
$+\frac{1}{Z_d^2}(\mathrm{e}^{-\beta(2(\varepsilon_d-\mu)+U_d)} + \mathrm{e}^{-2\beta(\varepsilon_d-\mu)})\left[\frac{1}{(\mathrm{i}\omega_\nu-U_d)} + \frac{1}{(\mathrm{i}\omega_\nu+U_d)}\right]$

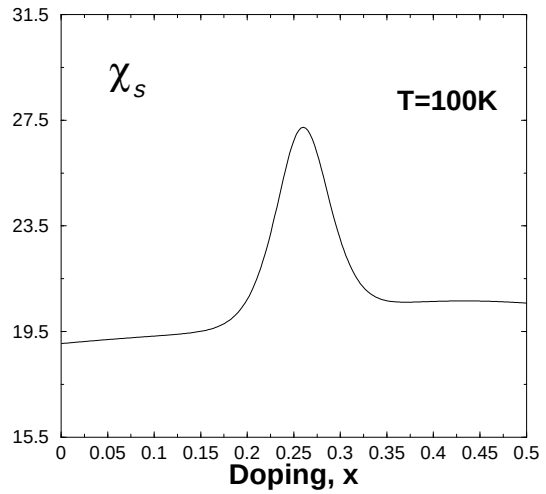

Fig. 8. The spin magnetic susceptibility $\chi_{\mathrm{s}}(\mathbf{0},0)$ (in unit of V^{-1}) as a function of the doping x, for the same parameters as in Figure 1.

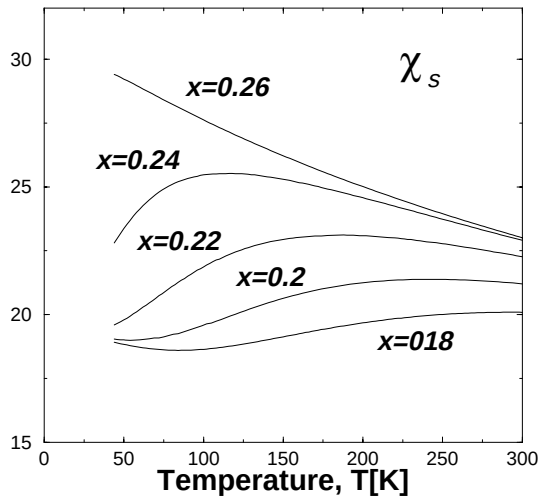

Fig. 9. The spin magnetic susceptibility $\chi_{\mathrm{s}}(\mathbf{0},0)$ (in unit of V^{-1}) as a function of the temperature T for various values of the doping $x < x_{\mathrm{c}}$ and $U_d/V = 5$, $\varepsilon_d/V = -1$.

correlated with the half-filling point, but occurs at a finite doping, depending on the interaction U_d/V. In the approximation in which only first-order cumulants are taken into account in the resummation of the Dyson equation for the Green's functions, the effect of the correlation U_d is essentially that of distributing the spectral weight determined by the hybridization V_{pd} with a consequent shift of the Fermi level with respect to the Van Hove singularity. Other effects of the correlation (such as the formation of the Zhang-Rice singlets) will appear only when higher-order cumulants or corrections to the self-energy are taken into account.

We would like to stress that the parameters U_d and ε_d have been fixed to fit the experimental results observed in $La_{2-x}Sr_xCuO_4$ [1], anyway in the following discussion the behavior of the physical quantities remains qualitatively the same at varying U_d/V and ε_d/V, apart the value of x_{c} which may differ significantly from that observed experimentally.

Let us discuss the numerical results for the static and uniform spin susceptibility $\chi_{\mathrm{s}}(\mathbf{0},0)$. The dependence on x of χ_{s} is depicted in Figure 8, for renormalized parameters $U_d/V = 5, \varepsilon_d/V = -1$ e $\varepsilon_p/V = 0$, while the temperature has been fixed at $T = 100$ K. As the system is doped away from half-filling ($x = 0$) the susceptibility increases, reaches a maximum at $x_{\mathrm{c}} \simeq 0.26$, then decreases. This behaviour is in qualitative agreement with experiments performed on various ceramic compounds, such as $La_{2-x}Sr_xCuO_4$ [1,2] and $YBa_2Cu_3O_{6+x}$ [3], where a broad peak at $x \simeq 0.26$ is observed. The $x-$dependence of the spin magnetic susceptibility can be explained according to a Van-Hove scenario [11,23]. Since χ_{s} reflects the thermal average of the density of states at the Fermi level $N(E_{\mathrm{F}})$, the presence of a maximum in χ_{s} for the critical doping x_{c} can be related to the fact that, upon doping with holes, the Fermi level approaches the Van Hove singularity (VHS) arising from the nearest-neighbour hybridization term, and lies on it at $x = x_{\mathrm{c}}$. Interpretation of the experimental results obtained in reference [1] for LSCO in terms of a sharp feature in the density of states, consistent with photoemission spectroscopy data on cuprates [8,9], has been primarily advanced by Thoma *et al.* [24]. The consistency of the thermodynamical data with the presence of a VHS near the Fermi level was also shown by Newns *et al.* [23] by considering a *p-d* like model in the framework of the slave-boson mean-field theory in the limit of large U.

To have a better understanding of the change of χ_{s} with doping, in Figures 9 and 10 we report $\chi_{\mathrm{s}}(T)$ *versus* temperature for different values of the doping x.

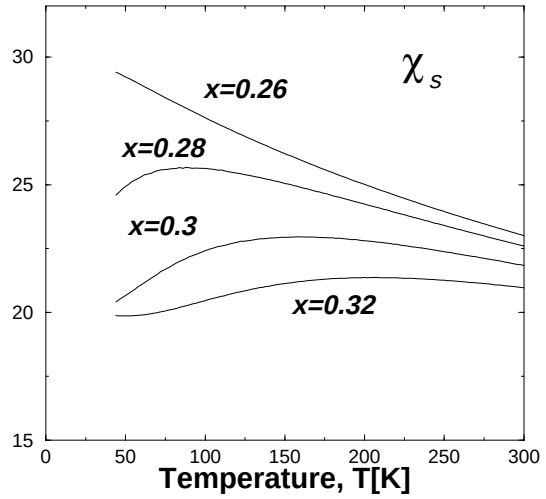

Fig. 10. The spin magnetic susceptibility $\chi_{\rm s}(\mathbf{0},0)$ (in unit of V^{-1}) as a function of the temperature T for various values of the doping $x > x_{\rm c}$ and $U_d/V = 5$, $\varepsilon_d/V = -1$.

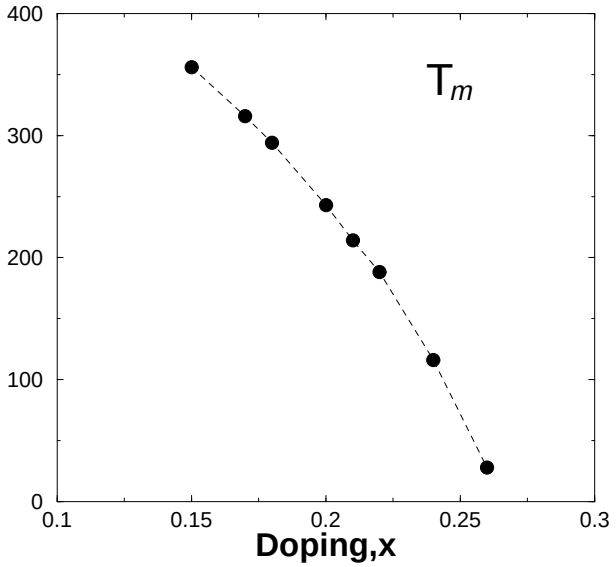

Fig. 11. The temperature $T_{\rm m}$ (in kelvin), where $\chi_{\rm s}(\mathbf{0},0)$ has a maximum, reported as a function of the doping x, for $U_d/V = 5$ and $\varepsilon_d/V = -1$. The behavior of $T_{\rm m}$ is very similar to the experimental results from reference [1].

As shown, upon doping with holes $\chi_{\rm s}(T)$ increases till a critical value $x_{\rm c}(\simeq 0.26)$ and then behaves in the reverse for $x \geq x_{\rm c}$. This behavior well reproduces the experimental data from reference [1]. Finally, as a function of T, in the high-temperature region $\chi_{\rm s}$ exhibits a Curie-like behaviour. On the other hand, in the low-temperature region an upturn in $\chi_{\rm s}$ occurs for $x \simeq 0.26$, while a downturn is achieved for $x \neq x_{\rm c} = 0.26$. The upturn in $\chi_{\rm s}(T)$ at low T indicates the influence of the VHS in the density of states when the Fermi-level $E_{\rm F}$ is very close to the singularity. By contrast, when x is different from $x_{\rm c}$, $E_{\rm F}$ lies away from the VHS and the contribution of the density of states to the spin susceptibility decreases as the temperature is lowered. The temperature of the maximum $T_{\rm m}$ as a function of the doping decreases at increasing doping, tending to zero at the critical doping $x_{\rm c}$. This is illustrated in Figure 11 where $T_{\rm m}$ is plotted as a function of x. Our theoretical results qualitatively reproduce the experimental results for $La_{2-x}Sr_xCuO_4$ [1,2] and $YBa_2Cu_3O_{6+x}$ [3].

5 Summary and discussion

We have investigated the doping and the temperature dependence of the spin susceptibility in the p-d model, by using a generalized cumulant expansion which seems appropriate to study physical quantities in the optimal and overdoped region. In the study of the spin susceptibility, at varying doping, an upturn or a downturn in $\chi_{\rm s}$ is achieved as T is lowered, whose origin is ascribed to a band effect such as VHS, in combination with the shift of the Fermi level with respect to it, due to electron correlations: it has been pointed out that the DOS has a peak near the Fermi level due to a VHS for a finite value of the doping and this peak runs away from the Fermi level as $x \to 0$. The results show that upon doping with holes, $\chi_{\rm s}$ exhibits a maximum at a certain critical value $x_{\rm c}$, at a fixed temperature. As a function of temperature the magnitude of $\chi_{\rm s}$ increases with doping and exhibits a maximum that broadens and shifts to lower temperature for $x \leq x_{\rm c}$. The opposite behaviour is observed for $x > x_{\rm c}$. It is worth stressing that at the critical doping $x_{\rm c}$ the Fermi level lies on a Van Hove singularity in the density of states.

In conclusion, in the framework of the $p-d$ model a Van Hove scenario describes well some of the "unusual" magnetic properties observed in the normal state of HTCS, in particular when approaching the analysis from the paramagnetic metallic phase (large x) rather than the antiferromagnetic (AF) phase and the theoretical results qualitatively reproduce the experimental scenario for $La_{2-x}Sr_xCuO_4$ [1,2] and $YBa_2Cu_3O_{6+x}$ [3]. Anyway, at low doping the presented perturbation approach underrates $p-d$ spin fluctuations *a la* Zhang-Rice which dominate the physics in the quasi-atomic limit, and the simple Van Hove scenario is not sufficient to describe the physics of cuprates. In this region the natural starting point would be the inclusion of the spin-fluctuations' corrections to the self-energy. Results concerning this point require rather long analytical and numerical calculations and will be reported elsewhere. Nonetheless, preliminary results indicate that the AF spin-exchange affects the structure of the Van Hove singularity leading to an opening of a pseudogap in the density of states, near the chemical potential, that varies with doping and temperatures. Work is in progress along this line.

References

1. J.B. Torrance *et al.*, Phys. Rev. B **40**, 8872 (1989).
2. T. Nakano *et al.*, J. Low Temp. Phys. **105**, 395 (1996).
3. D.C. Johnston *et al.*, Physica C **153-55**, 572 (1988).

4. W.C. Lee *et al.*, Phys. Rev. Lett. **63**, 1012 (1989).
5. Y. Koike *et al.*, in *Mechanism of Superconductivity*, JJAP Series 7, edited by Y. Muto (1992), p. 225.
6. Y. Kitaoka *et al.*, J. Phys. Chem. Solids **54**, 1385 (1993).
7. M. Takigawa *et al.*, Phys. Rev. B **40**, 247 (1991).
8. D.S. Dessau *et al.*, Phys. Rev. Lett. **71**, 2781 (1993).
9. K. Gofron *et al.*, J. Phys. Chem. Solids **54**, 1193 (1993); K. Gofron *et al.*, Phys. Rev. Lett. **73**, 3302 (1994).
10. R.S. Markiewicz, J. Phys.-Cond. **2**, 6223 (1990); R.S. Markiewicz, `cond-mat/9611238`.
11. E. Dagotto *et al.*, Phys. Rev. Lett. **74**, 310 (1995).
12. D.S. Marshall *et al.*, Phys. Rev. Lett. **76**, 4841 (1996).
13. M. Ding *et al.*, Nature **382**, 51 (1996).
14. J. Friedel, J. Phys.-Cond. **1**, 7757 (1989).
15. A.V. Mahajan, H. Alloul, G. Collin, J.F. Marucco, Phys. Rev. Lett. **72**, 3100 (1994).
16. A.M. Olés, J. Zaanen, Phys. Rev. B **39**, 9175 (1989).
17. T. Hotta, S. Fujimoto, Phys. Rev. B **54**, 5381 (1996).
18. W. Metzner, Phys. Rev. B **43**, 8549 (1991).
19. M. Marinaro, C. Noce, A. Romano, J. Phys.-Cond. **3**, 3719 (1991).
20. A. Romano, C. Noce, R. Citro, Solid State Commun. **104**, 623 (1997).
21. R. Citro, M. Marinaro, Z. Phys. B **103**, 153 (1997).
22. F. Mancini, M. Marinaro, Y. Nakano, Physica B **159**, 330 (1989).
23. D.M. Newns *et al.*, Phys. Rev. B **43**, 3075 (1991).
24. J. Thoma *et al.*, Phys. Rev. B **51**, 15393 (1995).